APPENDIX 2

Influence of Oceanic Whitecaps on Atmospheric Correction of SeaWIFS

by

Howard R. Gordon and Menghua Wang

When this work was performed, the authors were with the Department of Physics, University of Miami, Coral Gables, FL 33124. M. Wang is now with Research and Data Systems Corporation, 7855 Walker Drive, Greenbelt, MD 20770.

(Submitted to *Applied Optics*)

Acknowledgement

We are grateful to K. Ding for carrying out the Monte Carlo simulations in Appendix I and to the National Aeronautics and Space Administration for support under Grant NAGW-273 and Contracts NAS5-31363 and NAS5-31743.

Abstract

The effects of oceanic whitecaps on ocean color imagery is simulated and inserted into the Sea-viewing Wide-Field-of-View Sensor (SeaWiFS) atmospheric correction algorithm to understand its tolerance to errors in the estimated whitecap contribution. The results suggest that for wind speeds $\lesssim 10-12$ m/s present models relating whitecap reflectance to wind speed are sufficiently accurate to meet the SeaWiFS accuracy goal for retrieval of the water-leaving radiance in the blue when the aerosol scattering is weakly dependent on wavelength. In contrast, when the aerosol scattering has a strong spectral signature the retrievals will meet the goal only when the whitecap reflectance is underestimated.

Introduction

The Sea-viewing Wide-Field-of-View Sensor[1] (SeaWiFS) for studying oceanic primary productivity through observations of ocean color is scheduled for launch in mid 1994. This scanning radiometer's heritage was the Coastal Zone Color Scanner[2,3] (CZCS), which provided ocean color imagery from 1978 to 1986. Since $\sim$ 80 to 100% of the radiance exiting the top of the atmosphere over the oceans in the visible is the result of scattering in the atmosphere, isolating the radiance exiting the ocean (the "ocean color") requires accurate removal of the atmospheric contamination. This is termed atmospheric correction.

In a recent paper, we presented an algorithm for the atmospheric correction of SeaWiFS.[4] Briefly, the total radiance $L_t^{(m)}(\lambda)$ measured at the top of the atmosphere at a wavelength λ can be decomposed as follows:

$$L_t^{(m)} = L_r + L_a + L_{ra} + tL_{wc} + tL_w, \tag{1}$$

where L_r is the radiance resulting from multiple scattering by air molecules (Rayleigh scattering) in the absence of aerosols, L_a is the radiance resulting from multiple scattering by aerosols in the absence of the air, L_{ra} is the interaction term between molecular and aerosol scattering,[5] $L_{wc}(\lambda)$ is the radiance at the sea surface arising from sunlight and skylight reflecting from individual whitecaps on the surface, and $L_w(\lambda)$ is the desired water-leaving radiance, i.e., the radiance exiting the ocean. Note, both L_{wc} and L_w are measured at the sea surface. Radiance arising from specular reflection of direct sunlight from the sea surface (sun glitter) has been ignored because SeaWiFS can be tilted away from the glitter pattern. In this equation, t is the diffuse transmittance of the atmosphere. The diffuse transmittance for a viewing angle θ_v with respect to the nadir is approximated by

$$t(\theta_v) = \exp\Big[-\Big(\frac{\tau_r}{2} + \tau_{Oz}(\lambda)\Big)\Big(\frac{1}{\mu_v}\Big)\Big] t_a(\theta_v), \tag{2}$$

where

$$t_a(\theta_v) = \exp\Big[-\frac{[1-\omega_a F_a(\mu_v)]\tau_a}{\mu_v}\Big], \tag{3}$$

$\mu_v = \cos\theta_v$, τ_r, τ_{Oz}, and τ_a are, respectively, the Rayleigh, Ozone, and aerosol optical thicknesses, and ω_a is the aerosol single scattering albedo. $F_a(\mu_v)$ is related to the scattering phase function of the aerosol and is given by

$$F_a(\mu_v) = \frac{1}{4\pi}\int_0^1 P_a(\alpha)\, d\mu\, d\phi,$$

where $P_a(\alpha)$ is the aerosol phase function (normalized to 4π) for a scattering angle α, and

$$\cos\alpha = \mu\mu_v + \sqrt{(1-\mu^2)(1-\mu_v^2)}\cos\phi.$$

If θ_v is $\lesssim 60°$ the factor $[1-\omega_a F_a(\mu_v)]$ is usually $\ll 1$, so t_a depends only weakly on the aerosol optical thickness and this dependence is usually ignored. It is important to note that the diffuse transmittance takes into account the interaction between all of the light leaving the sea surface $L_w + L_{wc}$ and the atmosphere, e.g., when the sensor views a given pixel, it accounts for the light from that pixel transmitted through the atmosphere as well as the light from all the other pixels that is scattered into the field of view of the sensor, assuming that $L_w + L_{wc}$ is the same for all pixels. Equations (2) and (3) are exact in the single scattering approximation, i.e., when the exponentials are expanded and terms of second order or higher in the τ's can be ignored.

The goal of the atmospheric correction is the retrieval of L_w from $L_t^{(m)}$. It is convenient to convert radiance (L) to reflectance (ρ) defined to be $\pi L/F_0 \cos\theta_0$, where F_0 is the extraterrestrial solar irradiance, and θ_0 is the solar zenith angle. Then Eq. (1) becomes

$$\rho_t^{(m)}(\lambda) = \rho_r + \rho_a + \rho_{ra} + t\rho_{wc} + t\rho_w. \tag{4}$$

Our correction algorithm[4] ignored whitecaps, i.e., it assumes that the quantity $\rho_t = \rho_t^{(m)} - t\rho_{wc}$ is provided. It then utilizes ρ_t in the near infrared (NIR) at 765 and 865 nm, where ρ_w can be taken to be zero, to choose an aerosol model from a set of candidate models. This aerosol model is then used to predict $\rho_a + \rho_{ra}$ in the visible, which when combined with ρ_r, yields the desired $t\rho_w$. To assess the efficacy of the algorithm, we simulated ρ_t using aerosol models which were similar, but not identical, to the candidate aerosols models. The simulated ρ_t was used as pseudodata for insertion into the correction algorithm. The error $\Delta\rho$ in the retrieval of $t\rho_w$ at 443 nm was nearly always found to be $\lesssim 0.002$ and often $\lesssim 0.001$. This meets the SeaWiFS goal of retrieving L_w at 443 nm to within $\pm 5\%$ in waters with low phytoplankton pigment concentrations (C), e.g., the Sargasso Sea in summer.

Operation of the algorithm requires estimation of ρ_{wc} to convert $\rho_t^{(m)}$ to ρ_t. In this paper we will estimate the influence of error in ρ_{wc} on the retrieved ρ_w.

Whitecaps

It is useful to define the normalized water-leaving radiance,[6] $[L_w]_N$, according to

$$L_w(\lambda) = [L_w(\lambda)]_N \cos\theta_0\, t(\theta_0, \lambda). \tag{5}$$

The normalized water-leaving radiance is approximately the radiance that would exit the ocean in the absence of the atmosphere with the sun at the zenith. It has proved useful in the analysis of ocean color imagery because for $\lambda \gtrsim 520$ nm it is nearly independent of C for $C \lesssim 0.3$ mg/m^3. The normalized water-leaving radiance can easily be converted to normalized water-leaving reflectance $[\rho_w]_N$ through

$$[\rho_w]_N = \frac{\pi}{F_0}[L_w]_N,$$

and Eq. (5) becomes

$$\rho_w(\lambda) = [\rho_w(\lambda)]_N \, t(\theta_0, \lambda). \tag{6}$$

As in the case of the normalized water-leaving radiance, we define the normalized whitecap reflectance (or the albedo) $[\rho_{wc}]_N$ to be the average reflectance of the ocean surface (over several pixels) *at* the sea surface resulting from the whitecaps in the absence of the atmosphere. Then the radiance leaving the surface from whitecaps is

$$L_{wc}(\lambda) = [\rho_{wc}(\lambda)]_N \frac{F_0 \cos\theta_0}{\pi} \, t(\theta_0, \lambda),$$

where the whitecaps are assumed to be lambertian. Converting to reflectance we have

$$\rho_{wc}(\lambda) = [\rho_{wc}(\lambda)]_N \, t(\theta_0, \lambda),$$

which is similar in form to Eq. (6). At the top of the atmosphere, the whitecaps contribute

$$t\rho_{wc}(\lambda) = [\rho_{wc}(\lambda)]_N \, t(\theta_0, \lambda) t(\theta_v, \lambda).$$

The problem to be faced in removing $t\rho_{wc}$ from $\rho_t^{(m)}$ is the estimation of $[\rho_{wc}]_N$.

It is obvious that the fraction of the sea surface covered with whitecaps is related to the wind speed W; however, it is also related to the atmospheric stability,[7,8] and possibly to the water temperature itself.[9] If T_A and T_W are the air and water temperatures, respectively, then a measure of the stability is the air-sea temperature difference $\Delta T = T_A - T_W$, with $\Delta T > 0$ implying a stable atmosphere. Unfortunately, $[\rho_{wc}]_N$ has not been related to these quantities directly. Rather, the fraction f of the sea surface covered by whitecaps is usually related to W, ΔT, and T_W. The reflectance $[\rho_{wc}]_N$ is then taken to be f times r_{wc}, the effective reflectance of a whitecap.[10,11] For the spectral range of interest to SeaWiFS the effective reflectance is almost independent[12] of λ and has been determined by Koepke[11] to be $\sim 22\%$. To estimate $[\rho_{wc}]_N$ Koepke used a statistical expression derived by Monahan and O'Muircheartaigh[13] summarizing the very noisy relationship between f and W:

$$f = 2.95 \times 10^{-6} \, W^{3.52},$$

where W is in m/s. Later Monahan and O'Muircheartaigh[14] modified the expression to

$$f = 1.95 \times 10^{-5}\, W^{2.55} \exp[-0.0861 \Delta T],$$

which included the influence of the atmospheric stability. Using Koepke's effective reflectance we have computed $[\rho_{wc}]_N$ as a function of the wind speed and stability (Figure 1). The two expressions give qualitatively similar values of $[\rho_{wc}]_N$. A variation in ΔT of $\pm 5°C$ would appear to cause a variation in $[\rho_{wc}]_N$ of $\sim \pm 0.001$ when $W \sim 12$ m/s. For reference, the *annual mean* of ΔT is -0.1 to $-1.5°C$, and the *annual mean* wind speeds are between 5 and 9 m/s.[15]

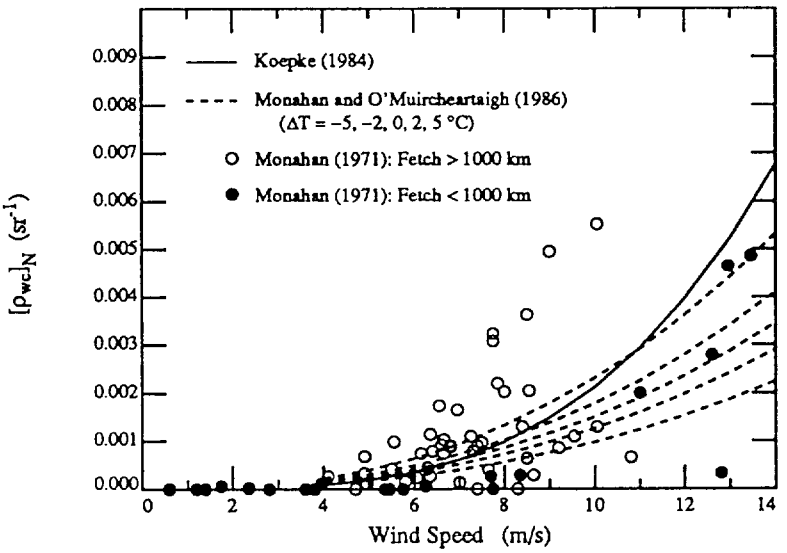

Figure 1. $[\rho_{wc}]_N = r_{wc} f$ as a function of wind speed and atmospheric stability. For the Monahan and O'Muircheartaigh[14] relationship, the lower the value of $[\rho_{wc}]_N$ the greater the stability of the atmosphere.

To provide an appreciation for the variance in the $[\rho_{wc}]_N$ vs. W relationship, Figure 1 also includes experimental results from one data set.[8] These data for f have been converted to $[\rho_{wc}]_N$ by assuming a whitecap effective reflectance of 22%. The result clearly shows that the mean $[\rho_{wc}]_N$ can be expected to have a standard deviation approximately equal to the mean itself, i.e., for a given $W \lesssim 10$ m/s $[\rho_{wc}]_N$ can range from 0 to approximately twice the mean. Other data sets are similar, e.g., see Monahan and O'Muircheartaigh.[13]

From the data presented by Bortkovskii,[9] there appears to also be a dependence on the water temperature itself; however, as pointed out by Monahan and O'Muircheartaigh,[14] it is not clear if the effect is real or due to the fact that the cold water measurements may not be representative because the seas may not have been fully developed in regions where such measurements have been made. For fully developed seas, $f \sim W^{\eta}$, and for nonfully developed seas the value of η is reduced. Thus, the value of the exponent depends in some manner on the "duration" of the wind in the open ocean (where there is no fetch limitation).

Whitecap Influence on L_w Retrieval

In this section we examine the influence of whitecaps on the accuracy of the ρ_w retrieval. For simplicity we take $\rho_w = 0$ at all wavelengths. As before, we will indicate the reflectance measured at the top of the atmosphere as $\rho_t^{(m)}$. The measured reflectance consists of two parts, that which would be measured in the absence of whitecaps and the reflectance added by the whitecaps $t\rho_{wc}$, i.e.,

$$\rho_t^{(m)} = \rho_t + t\rho_{wc}. \tag{7}$$

In the computation of t, t_a is set equal to unity for simplicity. The validity of this equation is discussed in Appendix I. The ρ_w retrieval algorithm must be operated with ρ_t rather than $\rho_t^{(m)}$, thus it is necessary to estimate the whitecap reflectance ρ_{wc}. This is accomplished by using W, ΔT, and T_W as discussed above. However, since the relationship between ρ_{wc} and these parameters is only poorly established and very noisy (Figure 1), there can be considerable error in the estimated ρ_{wc}. Thus, we need to know the influence of an error in ρ_{wc} on the ρ_w retrieval. We can understand how the error propagates through the algorithm by considering single scattering. Assuming that the single scattering algorithm provided in Appendix II is exact,

$$t(\lambda_i)\rho_w(\lambda_i) = \rho_t(\lambda_i) - \rho_r(\lambda_i) - \varepsilon(\lambda_i, \lambda_l)\left[\rho_t(\lambda_l) - \rho_r(\lambda_l)\right], \tag{8}$$

where λ_i is the wavelength of the band for which we want to retrieve ρ_w, and λ_l is the longer of the two NIR bands. Now, we use $\rho_t^{(m)}$ in the algorithm rather than ρ_t, but try to correct it for the presence of whitecaps by subtracting off an estimate of ρ_{wc}, which we refer to as $\rho_{wc}^{(e)}$. Then, letting

$\rho'_w(\lambda_i)$ represent the resulting value of $\rho_w(\lambda_i)$ when the algorithm is operated with $\rho_t^{(m)} - t\rho_{wc}^{(e)}$ in place of ρ_t, we have

$$t(\lambda_i)\rho'_w(\lambda_i) = \rho_t^{(m)}(\lambda_i) - t(\lambda_i)\rho_{wc}^{(e)}(\lambda_i) - \rho_r(\lambda_i) - \varepsilon^{(e)}(\lambda_i,\lambda_l)\left[\rho_t^{(m)}(\lambda_l) - t(\lambda_l)\rho_{wc}^{(e)}(\lambda_l) - \rho_r(\lambda_l)\right]. \quad (9)$$

Note that since the whitecaps also add radiance to the NIR bands, the extrapolated value of ε will be incorrect. We have indicated the incorrectly estimated value of ε by $\varepsilon^{(e)}$. Combining Eqs. (7) and (8) and noting that $t(\lambda)$ in Eq. (9) is really $t(\theta_v,\lambda)$, that $\rho_{wc}(\lambda) = t(\theta_0,\lambda)[\rho_{wc}(\lambda)]_N$, that $[\rho_{wc}(\lambda)]_N$ is independent of λ, and writing $\varepsilon^{(e)}(\lambda_i,\lambda_l) = \varepsilon(\lambda_i,\lambda_l) + \Delta\varepsilon(\lambda_i,\lambda_l)$, we have

$$\Delta\rho = -\Delta\rho_{wc}\left[\varepsilon^{(e)}(\lambda_i,\lambda_l)t(\theta_v,\lambda_l)t(\theta_0,\lambda_l) - t(\theta_v,\lambda_i)t(\theta_0,\lambda_i)\right] - \Delta\varepsilon(\lambda_i,\lambda_l)\left[\rho_t(\lambda_i) - \rho_r(\lambda_i)\right], \quad (10)$$

where $\Delta\rho \equiv t(\lambda_i)[\rho'_w(\lambda_i) - \rho_w(\lambda_i)]$, the error in the retrieved value of $t\rho_w(\lambda_i)$, and $\Delta\rho_{wc} \equiv [\rho_{wc}]_N - [\rho_{wc}]_N^{(e)}$, the error in the estimated value of $[\rho_{wc}]_N$. As mentioned above, the parameter $\varepsilon^{(e)}(\lambda_i,\lambda_l)$ is estimated from $\varepsilon^{(e)}(\lambda_s,\lambda_l)$, where λ_s is the shorter of the two NIR bands, by extrapolation. Because of whitecap influence in the NIR, $\varepsilon^{(e)}(\lambda_s,\lambda_l)$ will be in error by

$$\Delta\varepsilon(\lambda_s,\lambda_l) = [1 - \varepsilon(\lambda_s,\lambda_l)]\frac{X}{1+X}, \quad (11)$$

where we have taken $t(\lambda_s) = t(\lambda_l) = 1$ since τ_r and τ_a are both small in the NIR. The quantity X is defined to be $\Delta\rho_{wc}/[\rho_t(\lambda_l) - \rho_r(\lambda_l)]$, i.e., the ratio of the error in the whitecap reflectance to the reflectance caused by the aerosols at λ_l. Since ε is usually ≥ 1, $\Delta\varepsilon(\lambda_s,\lambda_l)$ and $\Delta\rho_{wc}$ will normally have opposite signs. Thus, $\Delta\varepsilon(\lambda_i,\lambda_l)$ will usually have a sign opposite to $\Delta\rho_{wc}$ and these two terms in Eq. (10) will tend to cancel.

It is illustrative to estimate $\Delta\rho$ for nadir viewing (scan center) with the sun near but not at the zenith (to avoid sun glint in the nadir view). In this case at $\lambda_i = 443$ nm, $t(\theta_0,443) \approx t(\theta_v,443) \approx 0.87$, and with $\lambda_l = 865$ nm, $t(\theta_0,865) \approx t(\theta_v,865) \approx 0.99$, so

$$\Delta\rho(443) \approx -\Delta\rho_{wc}\left[0.98\varepsilon^{(e)}(443,865) - 0.76\right] - \Delta\varepsilon(443,865)\left[\rho_t(\lambda_i) - \rho_r(\lambda_i)\right]. \quad (12)$$

Gordon and Wang[4] show that the values of $\varepsilon(443,865)$ range from $\sim$1 (for their Maritime models) to $\sim$2.5 (for their Tropospheric models). For the Maritime aerosol, the observed closeness of $\epsilon(\lambda_i,\lambda_l)$ to unity for all λ_i suggests that $\Delta\varepsilon(\lambda_i,\lambda_l) \approx 0$, so $\Delta\rho(443) \approx -0.22\Delta\rho_{wc}$, or typically,

$|\Delta\rho(443)| \ll |\Delta\rho_{wc}|$. In contrast, for the Tropospheric aerosol $\Delta\varepsilon(\lambda_s, \lambda_l)$ no longer vanishes and the term containing $\Delta\varepsilon(\lambda_i, \lambda_l)$ becomes very important, even dominant, because $\rho_t(\lambda_i) - \rho_r(\lambda_i)$ can be large in the blue due to the extreme spectral selectivity in aerosol scattering for this model. Thus, for these aerosols, it is possible that $|\Delta\rho(443)| > |\Delta\rho_{wc}|$. Clearly, whitecap effects are expected to be most important for aerosols with a strong spectral variation their in optical properties.

The derivation above is simply for the purpose of showing how the error propagates using a simplified algorithm. To provide quantitative estimates, we have carried out similar computations using the complete multiple scattering algorithm.[4] This was accomplished by simulating ρ_t for a totally absorbing ocean with a smooth Fresnel-reflecting surface, in the absence of whitecaps. The measured value of the reflectance is then $\rho_t^{(m)}$ in Eq. (7). Subtracting $t\rho_{wc}^{(e)}$ from both sides of Eq. (7) we obtain

$$\rho_t^{(m)} - t\rho_{wc}^{(e)} = \rho_t + t\Delta\rho_{wc} \equiv \rho_t^{(e)},$$

where $\rho_t^{(e)}$ is the estimated value of ρ_t after correcting for the presence of whitecaps. The estimated value $\rho_t^{(e)}$ is then used in place of ρ_t in the atmospheric correction algorithm and the error $\Delta\rho$ in the retrieved $t\rho_w$ at 443 nm is computed. The correction algorithm is an implementation of the algorithm provided in Ref. 4, with their Maritime, Coastal, and Tropospheric models at relative humidities (RH) of 50%, 70%, 90%, and 99% serving as twelve candidate aerosol models. The error in $t\rho_w$ at 443 nm, $\Delta\rho(443)$, was computed for the Maritime, Coastal, and Tropospheric models with RH = 80% (not one of the candidate aerosols) and for $\Delta\rho_{wc} = \pm 0.001, \pm 0.002$, and ± 0.004. The results are provided in Figures 2a–2f. For convenience we present the results for the Maritime and Tropospheric models at the scan center only. Note the expanded scale for $\Delta\rho$ for the Tropospheric cases (Figures 2b, 2d, and 2f). Also, in contrast to the single scattering analysis above, in which it was assumed that the correction algorithm itself was exact in the absence if whitecaps, the proposed SeaWiFS algorithm is not error free and in fact the error can be quite large, e.g., in the case of the Tropospheric aerosol. These simulations agree qualitatively with the single scattering model, i.e., the *additional* error induced by incorrectly assessing the whitecap reflectance is $\ll |\Delta\rho_{wc}|$ in the Maritime case and $\sim |\Delta\rho_{wc}|$ or larger in the Tropospheric case. However, they also provide a quantitative estimate of the *overall* error induced by the interaction of whitecaps *and* the correction algorithm.

Discussion

The simulations presented above suggest that in the case of an atmosphere with a Maritime aerosol, which shows little or no spectral selectivity in scattering, rather large errors in the estimated $[\rho_{wc}]_N$ can be tolerated. In fact, even for $\Delta\rho_{wc} = \pm 0.008$ (not presented) all of the retrieval errors $\Delta\rho = t\Delta\rho_w$, with the exception of one case, can be plotted on the same scale as Figures 2a, 2c, and 2e, i.e., $|\Delta\rho| \lesssim 0.002$. Note that $\Delta\rho$ includes the effect of errors in the correction algorithm itself. This robustness of the atmospheric correction algorithm to whitecap contamination owes to the fact that it treats whitecaps as aerosols, and since Maritime aerosols and whitecaps have similar spectral signatures, the whitecaps are removed along with the aerosol as long as $\Delta\rho_{wc}$ is not too large. However, since the correction algorithm tries to assess and account for multiple scattering, if ρ_{wc} becomes too large the assessment will be incorrect and a large $\Delta\rho$ will result.

In contrast to whitecaps, the Tropospheric aerosol has a strong spectral signature. When this aerosol is present the whitecaps reduce the apparent spectral signature of the aerosol and an incorrect model is chosen to assess the multiple scattering. This causes larger errors for the Tropospheric case compared to the Maritime aerosol. However, with the exception of $\theta_0 = 10°$, which will often be contaminated by sun glitter at the scan center, we find $|\Delta\rho| \leq 0.002$ as long as $|\Delta\rho_{wc}| < 0.004$ and $\theta_0 \leq 60°$. We note that it appears that in this case it is better to underestimate ρ_{wc} i.e., $\Delta\rho_{wc} > 0$. In fact, $\Delta\rho_{wc}$ can be as large as $+0.008$ and the error in $t\rho_w$ can still be plotted on the same scale as Figures 2b, 2d, and 2f.

The observations above suggest that a good strategy for dealing with whitecaps may be to underestimate somewhat their contribution to $\rho_t^{(m)}$. In fact, given the wind speed, if Koepke's estimate of $[\rho_{wc}]_N$ is chosen, and if the data in Figure 1 are representative, then with the exception of one data point ($W = 12.8$ m/s, $[\rho_{wc}]_N = 0.00025$ sr^{-1}), $-0.002 \lesssim \Delta\rho_{wc} \lesssim 0.0035$. For the Maritime aerosol case, $t\rho_w$ can be retrieved with an error less that $\lesssim \pm 0.001$ and with the exception of small solar zenith angles, the error is $\lesssim \pm 0.002$ for the Tropospheric aerosol for $\theta_0 \leq 60°$. Since underestimation of the whitecap contribution appears to be most important for aerosols that scatter with a strong spectral signature, it may be necessary to preprocess the

imagery to derive coarse values for $\varepsilon(\lambda_i, \lambda_l)$; i.e., to determine the spectral selectivity of the aerosol scattering, and to use this information to modify the relationship between $[\rho_{wc}]_N$ and W, ΔT, etc.

- It is interesting to note that the influence of the whitecaps is usually reduced at large solar zenith angles, e.g., $\theta_0 \gtrsim 60°$ (Figures 2b, 2d, and 2f). This is fortuitous, since the mean winds tend to be higher at higher latitudes.[15]

For highly reflecting waters a modification to the analysis is required. In particular, Eq. (7) should be replaced by

$$\rho_t^{(m)} = \rho_t + t\rho_{wc} - tf\rho_w,$$

where $tf\rho_w$ is the original contribution to the reflectance from areas that are now covered by whitecaps. The last term in this equation can be written

$$-t(\theta_v, \lambda_i)t(\theta_0, \lambda_i)f[\rho_w(\lambda_i)]_N$$

so there will be an additional error $-t(\theta_v, \lambda_i)t(\theta_0, \lambda_i)f[\rho_w(\lambda_i)]_N$ in the retrieval of $t\rho_w(\lambda_i)$. Note that we require that $[\rho_w]_N = 0$ in the NIR in order to effect atmospheric correction, so at 443 nm the above error is simply added to $\Delta\rho$ in Figure 2. In waters with very low C, $[\rho_w]_N$ can reach 0.04; however, it decreases rapidly with increasing C. So, typically the change in $|\Delta\rho|$ values at 443 nm from those in Figure 2 will be < 0.001 and usually $\ll 0.001$. In contrast, for highly reflecting waters, e.g., coccolithophore blooms for which it is possible for $[\rho_w]_N \approx r_{wc}$, the absolute error can be significantly higher; however, since the reflectance is proportionately higher, the tolerance on $|\Delta\rho|$ for recovering the water-leaving radiance within 5% is also proportionally higher.

Concluding Remarks

The simulations presented here suggest that present models of oceanic whitecaps, although very incomplete (Figure 1) may be good enough to allow retrieval of L_w from SeaWiFS imagery, in an atmosphere dominated by Maritime-like aerosols, with an accuracy within stated goals for wind speeds $\lesssim 10 - 12$ m/s. For an atmosphere dominated by Tropospheric-like aerosols (or any aerosol which scatters with a strong spectral signature), the simulations suggest that as long as the whitecap reflectance is not *overestimated*, the L_w accuracy goal can be met for $\theta_0 \lesssim 60°$; however,

the error is roughly twice a large as for the Maritime-like aerosol. Uncertainty in $[\rho_{wc}]_N$ may set the ultimate limit on the accuracy with which the water-leaving radiance can be retrieved from ocean color imagery.

A by product of our atmospheric correction algorithm is an estimate of the aerosol optical thickness. Our simulations suggest that $\tau_a = 0.05$ produces a reflection contribution $\rho_a + \rho_{ra}$ at 865 nm of between 0.004 and 0.008, depending on the aerosol type, e.g., Maritime or Tropospheric. Thus an error of ± 0.004 in $t\rho_{wc}$ would cause an error in τ_a of ± 0.025 to ± 0.05. Whitecap uncertainty probably sets the lower limit with which aerosol properties can be retrieved from satellite radiances.

Finally, it is important to note that the whitecap reflectance models used in this paper are based on subjective observations relating the fraction of sea surface covered by whitecaps to the wind speed, air-sea temperature difference, etc., and observations of the "mean" reflectance of individual whitecaps. We believe that it is important to test the efficacy of these models for predicting $[\rho_{wc}]_N$. This could be determined by measuring the reflectance enhancement by whitecaps using imaging radiometers operated from aircraft at high and low altitude.

Appendix I: Validity of Eq. (7)

Implicit in Eq. (7) is the assumption that all of the interaction between the whitecaps and the atmosphere can be described by the diffuse transmittances provided in Eqs. (2) and (3), and that t_a can be taken to be unity. To test this Monte Carlo simulations (with $\rho_w = 0$) were performed in which ρ_t, the ocean-atmosphere system reflectance with $f = 0$, and $\rho_t^{(m)}$ the reflectance in the presence of lambertian-reflecting whitecaps ($f = 0.02$), were computed. The value of $\rho_t^{(m)} - \rho_t$ was then compared with $t\rho_{wc}$, i.e., Eq. (7) with $t_a = 1$. The resulting error in the whitecap contribution using Eq. (7),

$$\delta \equiv \frac{t\rho_{wc} - (\rho_t^{(m)} - \rho_t)}{(\rho_t^{(m)} - \rho_t)} \times 100\%,$$

is provided in Table 1 for $\tau_a(865) = 0.2$, the Maritime aerosol model (RH = 80%), and nadir viewing. Clearly, Eq. (7) estimated the contribution of whitecaps to the reflectance at the top of

Table 1: % error in Eq. (7) at 443 and 865 nm.

θ_0	$\delta(443)$	$\delta(865)$	$\delta_a(443)$	$\delta_a(865)$
20°	−1.4	+7.6	− 4.5	+4.6
40°	−4.8	+5.4	−10.4	+1.8
60°	+0.4	+7.3	− 6.9	+0.5

the atmosphere with an error $\lesssim$ 10%. We also tested Eq. (7) with t_a given by Eq. (3). This led to the errors indicated by δ_a in Table 1. We note that the inclusion of t_a increases the error at 443 nm, but decreases it at 865 nm. Because of this, we let $t_a = 1$ for simplicity. A similar test for $\theta_0 = 80°$ was attempted; however, the Monte Carlo simulations could not be performed with sufficient accuracy to be able to estimate δ or δ_a. From Figure 1, for $f = 0.02$, $[\rho_{wc}]_N \approx 0.0044$, so the error in Eq. (7) is $\lesssim$ 0.0004 in the worst case for $\theta_0 \leq 60°$. Thus, our procedure for estimating $\rho_t^{(m)}$ should be accurate to within $\sim$ 0.0004 and often significantly more accurate.

Appendix II: Single scattering

In the single scattering approximation, i.e., in the approximation that photons can only scatter once in the atmosphere, the total reflectance at λ is given by

$$\rho_t(\lambda) = \rho_r(\lambda) + \rho_{as}(\lambda) + t(\lambda)\rho_w(\lambda), \tag{13}$$

where

$$\rho_{as}(\lambda) = \omega_a(\lambda)\tau_a(\lambda)p_a(\theta_v, \theta_0, \lambda)/4\cos\theta_v \cos\theta_0, \tag{14}$$

$$p_a(\theta_v, \theta_0, \lambda) = P_a(\theta_-, \lambda) + \Big(r(\theta_v) + r(\theta_0)\Big)P_a(\theta_+, \lambda),$$

$$\cos\theta_\pm = \pm\cos\theta_0\cos\theta_v - \sin\theta_0\sin\theta_v\cos(\phi_v - \phi_0),$$

and $r(\alpha)$ is the Fresnel reflectance of the interface for an incident angle α. The parameters $\tau_a(\lambda)$, $\omega_a(\lambda)$, and $P_a(\alpha, \lambda)$ are, respectively, the aerosol optical thickness, the aerosol single scattering albedo, and the aerosol scattering phase function for a scattering angle α. The angles θ_0 and ϕ_0 are, respectively, the zenith and azimuth angles of a vector from the point on the sea surface under examination (pixel) to the sun, and likewise, θ_v and ϕ_v are the zenith and azimuth angles of a vector from the pixel to the sensor. These are measured with respect to the *upward* normal so θ_v and θ_0 are both less than 90°. Note that we have ignored sun glitter and are assuming that the contribution from whitecaps has been subtracted from the measured reflectance to yield ρ_t.

Following the approach described in the text, we assume that $\rho_w = 0$ at two bands in the NIR at λ_s and λ_l, where the subscript "s" stands for short and "l" for long, e.g., for SeaWiFS $\lambda_s = 765$ nm and $\lambda_l = 865$ nm. Given estimates of the surface atmospheric pressure and the wind speed, $\rho_r(\lambda)$ can be computed essentially exactly and, therefore, $\rho_{as}(\lambda_s)$ and $\rho_{as}(\lambda_l)$ are determined from the associated measurements of $\rho_t(\lambda)$. This allows estimation of the parameter $\varepsilon(\lambda_s, \lambda_l)$:

$$\varepsilon(\lambda_s, \lambda_l) \equiv \frac{\rho_{as}(\lambda_s)}{\rho_{as}(\lambda_l)} = \frac{\omega_a(\lambda_s)\tau_a(\lambda_s)p_a(\theta_v, \theta_0, \lambda_s)}{\omega_a(\lambda_l)\tau_a(\lambda_l)p_a(\theta_v, \theta_0, \lambda_l)}. \tag{15}$$

If we can compute the value of $\varepsilon(\lambda_i, \lambda_l)$ for the SeaWiFS band at λ_i from the value of $\varepsilon(\lambda_s, \lambda_l)$, this will yield $\rho_{as}(\lambda_i)$, which, when combined with $\rho_r(\lambda_i)$, provides the desired $\rho_w(\lambda_i)$. The key to this procedure is the estimation of $\varepsilon(\lambda_i, \lambda_l)$ from $\varepsilon(\lambda_s, \lambda_l)$, which is usually effected by extrapolation according to some empirical "law," e.g., Gordon et al.[16] used $\varepsilon(\lambda_i, \lambda_l) = (\lambda_l/\lambda_i)^n$, while we[4] use aerosol models.

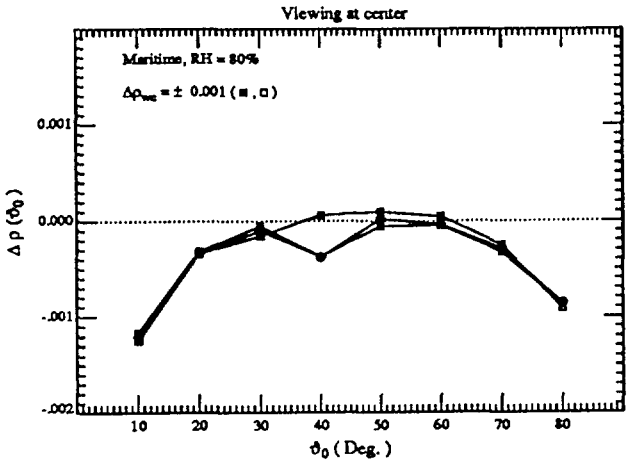

Figure 2a. Error in the retrieved $t(443)\rho_w(443)$ for viewing at the center the scan with a Maritime aerosol at RH = 80% as a function of the solar zenith angle with $\tau_a(865) = 0.2$ and an error of $\Delta\rho_{wc}$ in the estimation of ρ_{wc}. Solid circles are for $\Delta\rho_{wc} = 0$, solid squares are for $\Delta\rho_{wc} > 0$.

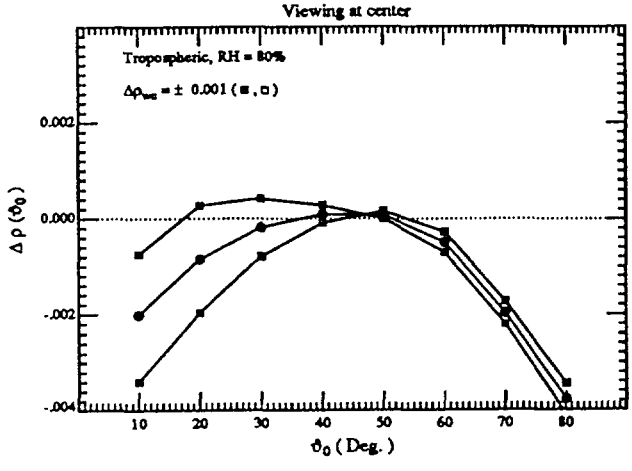

Figure 2b. Error in the retrieved $t(443)\rho_w(443)$ for viewing at the center the scan with a Tropospheric aerosol at RH = 80% as a function of the solar zenith angle with $\tau_a(865) = 0.2$ and an error of $\Delta\rho_{wc}$ in the estimation of ρ_{wc}. Solid circles are for $\Delta\rho_{wc} = 0$, solid squares are for $\Delta\rho_{wc} > 0$.

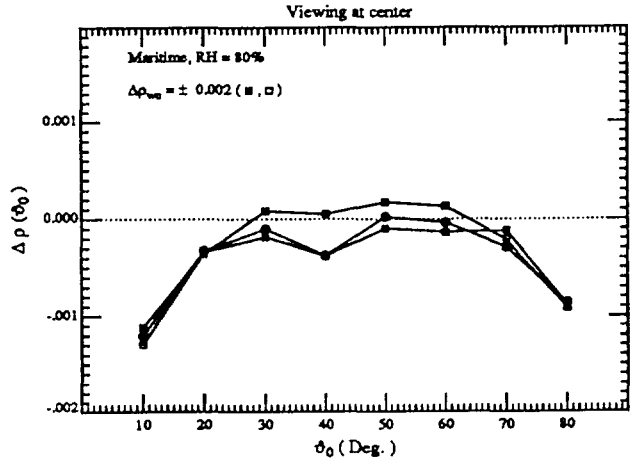

Figure 2c. Error in the retrieved $t(443)\rho_w(443)$ for viewing at the center the scan with a Maritime aerosol at RH = 80% as a function of the solar zenith angle with $\tau_a(865) = 0.2$ and an error of $\Delta\rho_{wc}$ in the estimation of ρ_{wc}. Solid circles are for $\Delta\rho_{wc} = 0$, solid squares are for $\Delta\rho_{wc} > 0$.

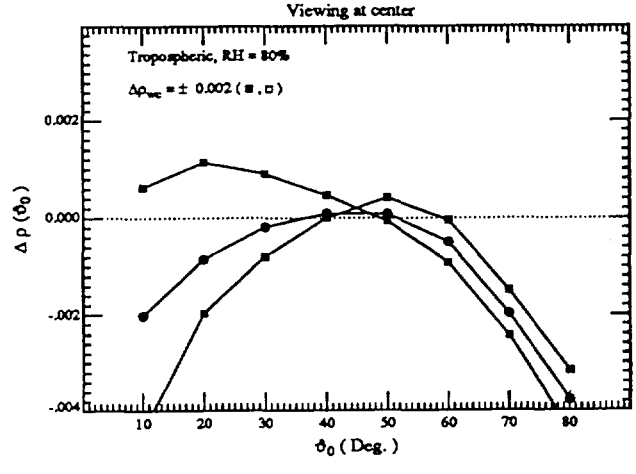

Figure 2d. Error in the retrieved $t(443)\rho_w(443)$ for viewing at the center the scan with a Tropospheric aerosol at RH = 80% as a function of the solar zenith angle with $\tau_a(865) = 0.2$ and an error of $\Delta\rho_{wc}$ in the estimation of ρ_{wc}. Solid circles are for $\Delta\rho_{wc} = 0$, solid squares are for $\Delta\rho_{wc} > 0$.

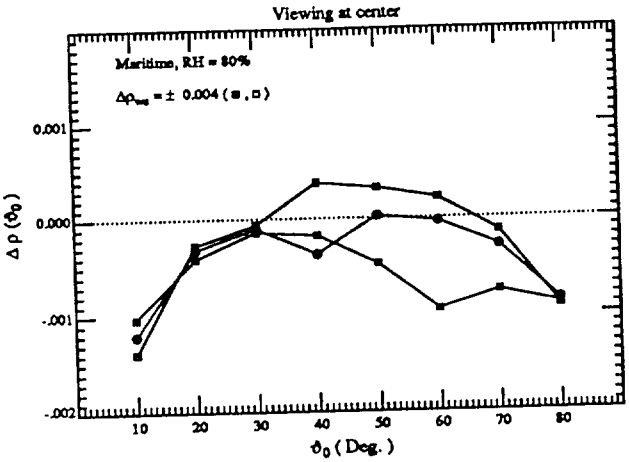

Figure 2e. Error in the retrieved $t(443)\rho_w(443)$ for viewing at the center the scan with a Maritime aerosol at RH = 80% as a function of the solar zenith angle with $\tau_a(865) = 0.2$ and an error of $\Delta\rho_{wc}$ in the estimation of ρ_{wc}. Solid circles are for $\Delta\rho_{wc} = 0$, solid squares are for $\Delta\rho_{wc} > 0$.

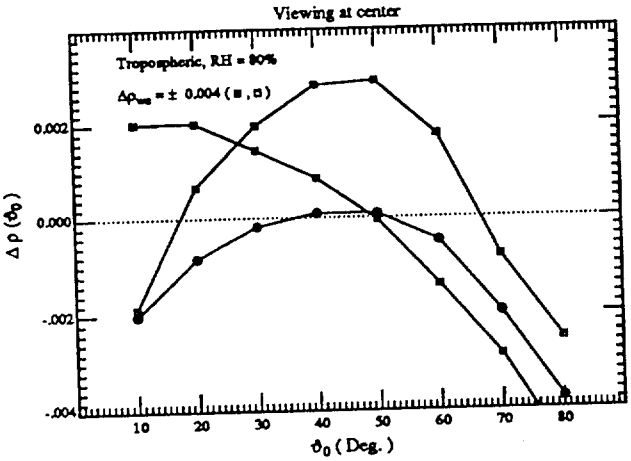

Figure 2f. Error in the retrieved $t(443)\rho_w(443)$ for viewing at the center the scan with a Tropospheric aerosol at RH = 80% as a function of the solar zenith angle with $\tau_a(865) = 0.2$ and an error of $\Delta\rho_{wc}$ in the estimation of ρ_{wc}. Solid circles are for $\Delta\rho_{wc} = 0$, solid squares are for $\Delta\rho_{wc} > 0$.

References

[1] S. B. Hooker, W. E. Esaias, G. C. Feldman, W. W. Gregg and C. R. McClain, *SeaWiFS Technical Report Series: Volume 1, An Overview of SeaWiFS and Ocean Color* (NASA Technical Memorandum 104566, July 1992).

[2] W. A. Hovis, D. K. Clark, F. Anderson, R. W. Austin, W. H. Wilson, E. T. Baker, D. Ball, H. R. Gordon, J. L. Mueller, S. Y. E. Sayed, B. Strum, R. C. Wrigley and C. S. Yentsch, "Nimbus 7 coastal zone color scanner: system description and initial imagery,"Science **210**, 60–63 (1980).

[3] H. R. Gordon, D. K. Clark, J. L. Mueller and W. A. Hovis, "Phytoplankton pigments derived from the Nimbus–7 CZCS: initial comparisons with surface measurements,"Science **210**, 63–66 (1980).

[4] H. R. Gordon and M. Wang, "Retrieval of water-leaving radiance and aerosol optical thickness over the oceans with SeaWiFS: A preliminary algorithm,"Applied Optics **32**, 0000–0000 (1993).

[5] P. Y. Deschamps, M. Herman and D. Tanre, "Modeling of the atmospheric effects and its application to the remote sensing of ocean color,"Applied Optics **22**, 3751–3758 (1983).

[6] H. R. Gordon and D. K. Clark, "Clear water radiances for atmospheric correction of coastal zone color scanner imagery,"Applied Optics **20**, 4175–4180 (1981).

[7] E. C. Monahan, "Fresh water whitecaps,"J. Atmos. Sci. **26**, 1026–1029 (1969).

[8] E. C. Monahan, "Oceanic Whitecaps,"J. Physical Oceanorgraphy **1**, 139–144 (1971).

[9] R. S. Bortkovskii, *Air-Sea Exchange of Heat and Moisture During Storms* (Reidel, Dordrecht, 1987), 194 pp.

[10] H. R. Gordon and M. M. Jacobs, "The Albedo of the Ocean-Atmosphere System: Influence of Sea Foam,"Applied Optics **16**, 2257–2260 (1977).

[11] P. Koepke, "Effective Reflectance of Oceanic Whitecaps,"Applied Optics **23**, 1816–1824 (1984).

[12] C. H. Whitlock, D. S. Bartlett and E. A. Gurganus, "Sea Foam Reflectance and Influence on Optimum Wavelength for Remote Sensing of Ocean Aerosols,"Geophys. Res. Lett. **7**, 719–722 (1982).

[13] E. C. Monahan and I. G. O'Muircheartaigh, "Optimal Power-Law Description of Oceanic Whitecap Coverage Dependence on Wind Speed,"J. Physical Oceanorgraphy **10**, 2094–2099 (1980).

[14] E. C. Monahan and I. G. O'Muircheartaigh, "Whitecaps and the passive remote sensing of the ocean surface,"Int. J. Remote Sensing **7**, 627–642 (1986).

[15] J. Hsiung, "Mean Surface Energy Fluxes Over the Global Ocean,"Jour. Geophys. Res. **91C**, 10,585–10,606 (1986).

[16] H. R. Gordon, D. K. Clark, J. W. Brown, O. B. Brown, R. H. Evans and W. W. Broenkow, "Phytoplankton pigment concentrations in the Middle Atlantic Bight: comparison between ship determinations and Coastal Zone Color Scanner estimates,"Applied Optics **22**, 20–36 (1983).